

## Electric discharge detection and localization using a distributed optical fiber vibration sensor



Igor Brutkowski Vieira da Costa<sup>a</sup>, Guilherme Heim Weber<sup>a</sup>, Danilo Fernandes Gomes<sup>a</sup>, José Rodolfo Galvão<sup>a</sup>, Marco J. da Silva<sup>a</sup>, Daniel R. Pipa<sup>a</sup>, Aritz Ozcariz<sup>b</sup>, Carlos R. Zamarreño<sup>b</sup>, Cicero Martelli<sup>a</sup>, Jean Carlos Cardozo da Silva<sup>a,\*</sup>

<sup>a</sup> Federal University of Technology-Parana (UTFPR), Curitiba 80230-901, Brazil

<sup>b</sup> Electrical and Electronic Engineering Department, Public University of Navarra, 31006 Pamplona, Spain

### ARTICLE INFO

**Keywords:**

Optical fiber sensor  
Distributed sensor  
Partial discharge  
Sagnac interferometry

### ABSTRACT

Partial discharges are a type of electric discharge that cause localized breakdowns in a small portion of an insulating material without forming a complete rupture. In high power electric machines as well as in transmission lines, partial discharges are caused by the degradation and/or the presence of defects in the insulation. The damage caused by the partial discharges can be either thermal, mechanical or chemical and can cause progressive deterioration of the insulation and lead to catastrophic failure causing serious safety risks. In this work a Distributed Optical Fiber Sensor System (DOFS) for vibration measurements based on Sagnac interferometry is proposed. This system uses acoustic wave emission phenomena to detect and locate electric discharges in electric machines and insulated electrical cables. Two experiments were carried out evaluating the performance of the system. Electric discharges were measured firstly over a conductive board with an attached 10 m long flat-coiled optical fiber sensor and secondly, over a 1.20 m long electrical cable with an optical fiber sensor longitudinally attached to it. Results demonstrate that due to the high sensitivity of the system it is possible to detect partial discharges in both proposed experiments. This effect is observed even with a theoretical fiber optical sensing spatial resolution of approximately 50 m.

### 1. Introduction

Partial discharges (PD) are a type of electric discharge that occurs in a region of space subjected to an electric field. The conductive path formed by the discharge does not completely connect the electric field poles [1]. Depending on their origin, partial discharges can be classified into three categories: surface discharges, corona discharges and internal discharges [2].

Surface discharges occur typically in gaseous and liquid media and cause changes on the surface of the dielectric material, forming conductive paths that propagate along the direction of the electric field [3]. This process can lead to a complete breakdown of the insulating material [2]. Surface-type discharges usually occur in shielded cables, terminations of cables, insulator skirts and end-windings of stator windings [1].

Corona discharges occur in gases and generate ozone and nitrogen oxides. These substances can cause cracking of the polymeric insulation and generate a corrosive product that can corrode metals and form

conductive deposits in the insulation of electrical cables [1,2].

Internal partial discharges occur in regions of low electrical resistance present in the solid materials used for high voltage insulation. Material defects such as gas filled regions in solid insulators are normally responsible for providing a low impedance path that gives rise to a discharge [1].

Partial discharges can produce audible or ultrasonic noise [4], light [5], gases and other substances, nonvisible electromagnetic waves [6], and high frequency current pulses [7].

Generally, a partial discharge appears as pulses of very short duration (much less than 1  $\mu$ s) and rise-times as short as 2 ns [8]. When a partial discharge occurs, the material is ionized around a hot spot. The ionization of the material causes an explosion generating mechanical energy which propagates as pressure waves [8]. The frequency of these waves varies from the audible range up to 200 kHz [4]. Typically, acoustic methods for partial discharge detection use the ultrasonic frequency range (approximately 20 kHz–250 kHz) as well as the audible range (100 Hz–20 kHz) [4,9].

\* Corresponding author.

E-mail address: [jeancs@utfpr.edu.br](mailto:jeancs@utfpr.edu.br) (J.C. Cardozo da Silva).

Several sensing methods based on optical fibers have been proposed in the literature. One example is acoustic fiber optical sensors, with the advantages of being highly sensitive and immune to electromagnetic interference [10]. The use of fiber optic sensors immersed in transformer oil has shown promising results in [11]. Sarkar et al. [12] describes the development of a sensor system for detecting partial discharges based on the use of optical fiber Bragg gratings (FBG). Other examples using fiber Bragg gratings are also demonstrated in [13,14].

In 2016, Rohwetter et al. [15] proposed the detection of partial discharges in splices of insulated high voltage cables by using an acoustic distributed optical fiber sensor system (DAS). In this system each splice of the high voltage cable was monitored by an optical fiber coil with about 30 m of fiber.

Interferometric optical fiber sensors for detecting ultrasonic waves have also been demonstrated. Posada-Roman et al. [16] demonstrated the detection of partial discharges in transformers using a Mach-Zehnder interferometer. Yu et al. [17] demonstrate the use of a sensor based on a Fabry-Perot interferometer for detecting partial discharges in transformers. In 2018, Wang et al. [18] proposed a system for detecting partial discharges through ultrasound emission analysis based on a Sagnac interferometer. This paper emphasizes the intrinsically safe detection of partial discharges in explosive atmospheres.

In the work presented here, we introduce the use of a distributed optical fiber sensor system based on Sagnac interferometry for the detection of electric discharges through vibration measurement. Differently than previously cited works, the proposed DOFS has the ability of monitoring the entire length of an instrumented electrical cable or an entire machine installed in a power plant with one single sensing system. Its construction is less complex when compared to Distribute Acoustic Sensor (DAS) systems as it is not based on light coherence.

Two experiments are carried out in order to demonstrate the feasibility of the sensor. First, a conductive board is instrumented with a 10 m long optical fiber flat coil and subjected to controlled electric discharges. This experiment simulates partial discharges in parts of electric machines such as stators of motors or generators and high voltage transformers. The second experiment consists of the monitoring of a 25 mm<sup>2</sup> cross section and 1.20 m in length insulated copper electrical cable. This cable was instrumented with a longitudinally attached optical fiber and exposed to electric discharges. Using this system, it was possible to identify and locate partial discharges in both experiments showing the technical potential of using the proposed system.

## 2. Principle of operation

The sensing principle combines optical time-domain reflectometry (OTDR) techniques integrated with a Sagnac interferometer as depicted in Fig. 1 and reported in [19]. The system consists of a modulated superluminescent light emitting diode (SLED) as optical source, an erbium-doped fiber amplifier (EDFA), a circulator, two optical couplers, a balanced photodiode and signal acquisition and processing tools. The amplified probe pulse is transmitted through the 50:50 wideband fiber coupler, OC<sub>1</sub>, where the signal is equally split into a delay fiber (DF) path of 1500 m and a second path of 2 m. The signals from the two paths are combined by the second 50:50 wideband fiber optic coupler,

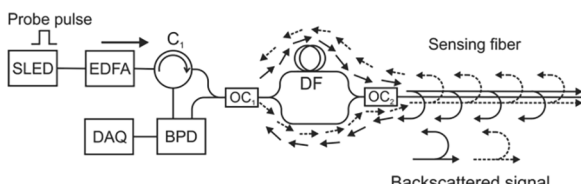


Fig. 1. Operating scheme of distributed optical fiber vibration sensor based on a Sagnac interferometer.

OC<sub>2</sub>, and launched into the 550 m sensing fiber. This topology allows two identical probe pulses into the sensing fiber, where the time interval between them is determined by the length difference of the two paths of the Sagnac interferometer.

There are four possible optical paths for the propagation of the pulse into the sensing fiber and the return of the backscattered light. In the shortest possible route, the light pulse travels through the shortest Sagnac path, enters the sensing fiber and the resulting backscattered light returns through the same path. In the second route, the longest, the pulse travels through the longest path of the Sagnac interferometer, enters the sensing fiber and returns through the same path. In the third route, the pulse propagates through the longest Sagnac path, enters the sensing fiber and the resulting backscattered light returns through the shortest path of the Sagnac interferometer. This route is illustrated by the continuous arrows in Fig. 1. In the fourth route, the pulse travels the shortest path and the backscattered light returns through the longest path. This is illustrated by the dashed lines (Fig. 1).

The last two optical routes mentioned have the same length. This allows two signals backscattered from the same position in the fiber that were originally traveling through the two different paths of the interferometer to interfere with each other at the coupler OC<sub>1</sub>. The light waves propagating along the third optical route can be defined as clockwise (CW) waves and the waves propagating along the fourth optical route can be defined as counterclockwise (CCW) waves [20]. The signal resulting from this optical interference is directly related to the difference in the backscattering light pattern between instants of time.

Thus, the desired information is carried by the backscattered signals from the CW and CCW waves. Pan et al. [19] and Wang et al. [21] demonstrated that the power of the detected signal corresponding to a position in the sensor fiber before any occurrence of vibrational disturbance is given by the equation:

$$P_b = K e^{-\alpha l} [1 + \cos(2\phi)] \quad (1)$$

where  $l$  is the fiber length,  $\alpha$  is the attenuation coefficient of the fiber,  $\phi$  is the phase shift induced by a mechanical disturbance in the fiber and  $K$  is a constant given by

$$K = \frac{1}{8} \alpha_s P_0 \quad (2)$$

where  $\alpha_s$  is the scattering coefficient of the fiber and  $P_0$  is the peak power of the input optical pulse.

When the sensing fiber is mechanically excited at a certain position, the backscattered signal corresponding to the fiber section beyond this position will experience a variation in phase given by the following equations [21]:

$$P_b(l) = K e^{-\alpha l} [1 + \cos[2\phi + 2\Delta\phi(l_v)]] \quad (3)$$

where  $l_v$  is the vibration position and the vibration-induced phase change  $\Delta\phi(l)$  is given by

$$\begin{aligned} \Delta\phi(l) &= \phi\left(\frac{l_v}{v_g}\right) + \phi\left(\frac{l_v}{v_g} + \Delta t_v(l)\right) - \phi\left(\frac{l_v}{v_g} + \Delta t_{DF}\right) - \phi\left(\frac{l_v}{v_g} + \Delta t_{DF} + \Delta t_v(l)\right) \end{aligned} \quad (4)$$

for  $l > l_v$ , where  $l$  is the fiber length,  $l_v$  is the vibration position,  $l_{DF}$  is the delay fiber length,  $v_g$  is the velocity of light in the fiber core,  $\Delta t_v(l) \approx \frac{l - l_v}{v_g}$  and  $\Delta t_{DF}(l) \approx \frac{l_{DF}}{v_g}$ .

The optical signals are transduced by a balanced photodetector and the resulting electronic signals are converted from analog to digital by a data acquisition system (DAQ) and it is further processed. The resulting backscattered signal is digitized at a sampling rate of 500 MS/s within a 14-bit resolution and analyzed by an algorithm in Matlab®.

### 3. Material and methods

Two experiments were proposed to evaluate and demonstrate the feasibility and performance of the sensor system as a tool for detecting partial discharges. The first experiment consists of a flat conductive board and a sharp electrode and the second involves an insulated electrical cable and the same sharp electrode.

The experiments were performed using a probe pulse 500 ns wide, at a repetition rate of 10 kHz, corresponding to a theoretical spatial resolution of approximately 50 m. The spatial resolution defines the length of fiber that an optical pulse occupies at a given time. Thus, the resulting signal of a given point disturbance spans the entire spatial resolution. In the experiments, the electric discharge is in the vicinity of a 10 m and a 1.2 m section of fiber, allowing the verification of this phenomenon.

#### 3.1. Electric discharges on a flat metal surface

A conductive flat copper board with an area of  $17 \times 19$  cm was instrumented with a fiber optical flat-coil sensor of 10 m and subjected to controlled electric discharges from the sharp electrode. This experiment can be correlated to partial discharges in electric machines such as stators of motors or generators and high voltage transformers.

A section of 10 m of the sensing fiber was glued to the board using cyanoacrylate in a spiral shape forming the flat-coil sensor, Fig. 2. The flat-coil sensor was made with a section of the sensing fiber located between 190 and 200 m, Fig. 4.

The board was subjected to electric discharges with an approximate duration of 1 s, voltage of 100 kV and frequency of 20 Hz in its central region. The electric power supply was a high voltage inverter.

#### 3.2. Electric discharges on an insulated electrical cable

In the second experiment, a  $25 \text{ mm}^2$  cross section, 1.20 m insulated cable was instrumented with fiber optics and subjected to electric discharges. Two sections of optical fiber with the same length were longitudinally placed between the insulation and the copper wires, as shown in Fig. 3.

The entire external and internal insulation jackets of the electrical cable have been longitudinally cut and the copper conductor removed. Two sections of the sensing fiber with the same length of the cable (1.2 m) were placed inside the insulation jacket and the copper conductor as replaced. The location of the first section of the sensing fiber placed inside the cable is approximately between 400 and 401.2 m, Fig. 4. The second section of the sensing fiber placed inside the cable is located approximately between 701.2 and 702.4 m, Fig. 4.

Electric discharges with the same characteristics as those presented in the first experiment (Section 3.1) were applied to the central length of the cable. The data acquisition and processing parameters were the same as used in the first experiment.

Figs. 4 and 5 show, respectively, the schematic and a picture of the

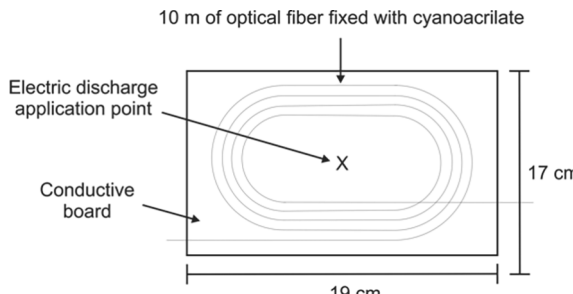


Fig. 2. Illustration of the conductive board instrumented with 10 m of fiber forming a spiral flat-coil sensor.

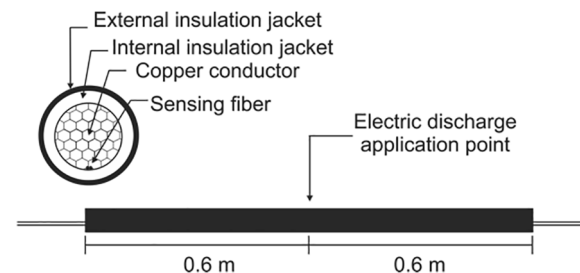


Fig. 3. Detail of the insulated electrical cable with two sensing fiber sections longitudinally placed between the insulation and the conductive copper wires.

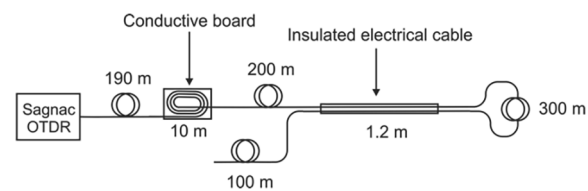


Fig. 4. Schematic representation of the experimental setup containing the conductive board and the electrical cable with fiber lengths.

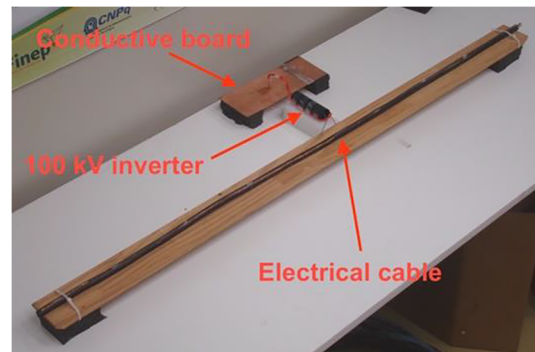
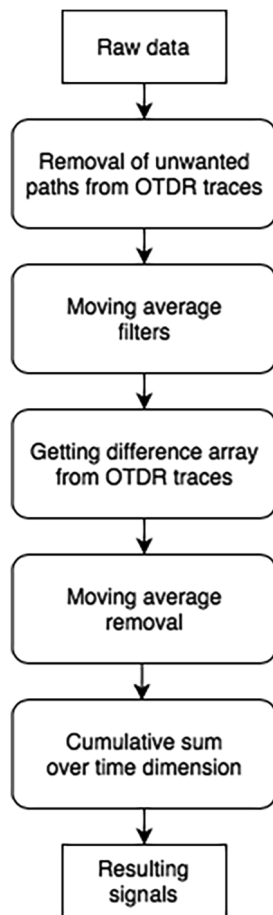


Fig. 5. Picture of the instrumented conductive board, instrumented insulated electrical cable and high voltage inverter.

entire test bed where the two experiments are carried out simultaneously using distinct positions of the sensing fiber. The conductive board is located between 190 and 200 m along the fiber and the two sections inside the electrical cable are located between 400 and 401.2 m and 701.2–702.4 m, respectively. Given the high sensitivity of the system to vibration, all fiber optical apart from the region of interest (i.e., conductive board and electrical cable) are kept inside of an acoustic insulated box (buffer sections of 190 m, 200 m, 300 m and 100 m represented in Fig. 4).

Fig. 6 presents a flow chart with the signal processing steps performed to obtain the resulting signals from raw data acquired using the optical fiber sensing system. Initially, the signals read from unwanted optical paths in each OTDR trace are removed from the raw data. The information is allocated in a two-dimensional matrix where the columns are the OTDR traces and the rows are the samples over time. Thus, the signal matrix can be converted into a fiber length vs. time signal. A moving average filter is applied in both spatial and temporal dimensions to reduce noise. A difference array is obtained by subtracting each OTDR trace from its spatial shifted image. The gauge length is defined by this shift, which is half of the pulse width converted to distance. This procedure allows the positions of fiber associated with the dynamic phase changes to be located. As a final step, a cumulative sum is performed over the temporal dimension. This procedure ensures the signal is proportional to the deformation.



**Fig. 6.** Processing steps to obtain the resulting signals from data acquired.

#### 4. Results and discussion

##### 4.1. Electric discharge on a flat metal surface

Fig. 7 demonstrates the electrical signal transduced by the photodetector acquired at different times during the electric discharge on metal surface experiment. The first 190 m of the sensing fiber is not exposed to the electric discharges, while the remainder is (Fig. 4). In the absence of vibration, and consequent stability of the backscattering of the sensing fiber, the measured signal is approximately constant. When an electric discharge is applied to the conductive board, the thermal expansions produced by these discharges cause mechanical waves. The signal transduced by the photodetector intrinsically reflects the accumulated phase change along the fiber under excitation. Amplitude remains constant for locations that do not undergo vibration (less than 190 m). At disturbed locations, the signal amplitude changes. The location of the electric discharge source can be directly identified from the interferometer (190 m).

In Fig. 8 it is possible to visualize the post-processed results for the experiments performed with the conductive board. Fig. 8(a) shows the demodulated signal in its representation in time, where the disturbances are evident from 900 ms to 1700 ms (approximate duration of the applied electric discharges, Section 3). This region coincides with the fiber section over the copper board. However, there is an uncertainty regarding the exact location of the sensed disturbances due to the signal spreading from approximately 170 m to 220 m. This is due to the 50 m value used for the gauge-length in processing, a value obtained from the theoretical resolution implied by the width of the probe pulse emitted by the SLED. The sensitivity of the system allows the identification of disturbances in lengths lower than the spatial

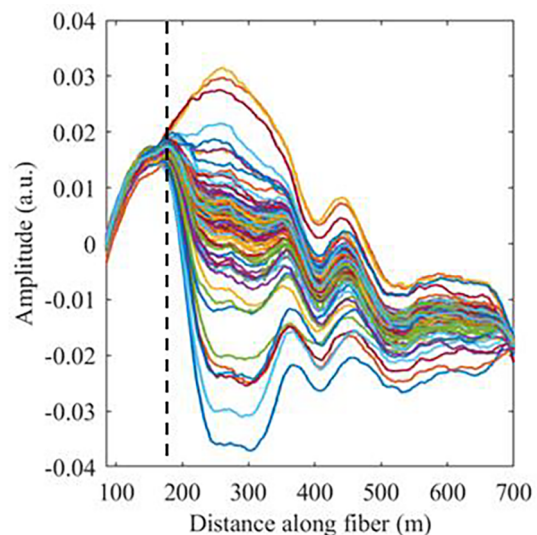


**Fig. 7.** Electrical signal transduced by the photodetector during the electric discharge on conductive board experiment. Each line represents the signal acquired at different instants of time demonstrating the sensing variation due to disturbances. Amplitude changes are seen after approximately 190 m. Before this location, the signal remains constant, showing the position subject to vibrations.

resolution, where the spatial resolution depicts merely the error on locating the disturbance source.

Fig. 8(b) demonstrates the power spectrum density (PSD) of the signal measured in the conductive board experiment. It can be seen that the mechanical vibration produced by the electric discharge and detected by the sensing fiber has most of its energy in low frequency components from 0 to 25 Hz.

##### 4.2. Electric discharge on an insulated electrical cable

The measured signal resulting from the partial discharges are presented in Fig. 9. The signal can be observed throughout the sensing fiber in the time domain, and Fig. 9(b) shows the signal in its representation in the frequency domain.

The plots show vibrations captured by the sensor system at two different points located at 400 m and 700 m along the fiber. As shown in Fig. 4 and explained in Section 3.2, these points correspond to the sections in which the optical fiber was longitudinally coupled to the electrical cable. Therefore, these results demonstrate the system's ability to detect and locate vibrations induced by electric discharges in electrical cables. In these locations, low frequency spectral components with emphasis on frequencies close to 22 Hz similarly to the results achieved in the first experiment and the high frequency inverter (Section 3.1) were found.

In addition to the highlighted frequencies associated with the locations related to the electrical cable, frequencies below 20 Hz show some source of vibration which is not associated with those induced by the electric discharges. The presence of this noise impairs the visualization of the induced electrical phenomenon in the time domain, Fig. 8(a). Hence, it is easier to visualize the discharges in the representation in the frequency domain.

Despite the noise in the frequency domain for frequencies below 20 Hz, a characteristic frequency signature response can be observed at 400 m and 700 m as highlighted in Fig. 9(b) as dashed lines. These harmonics occur at approximately 20 Hz and 40 Hz and are related to the discharge frequency (20 Hz).

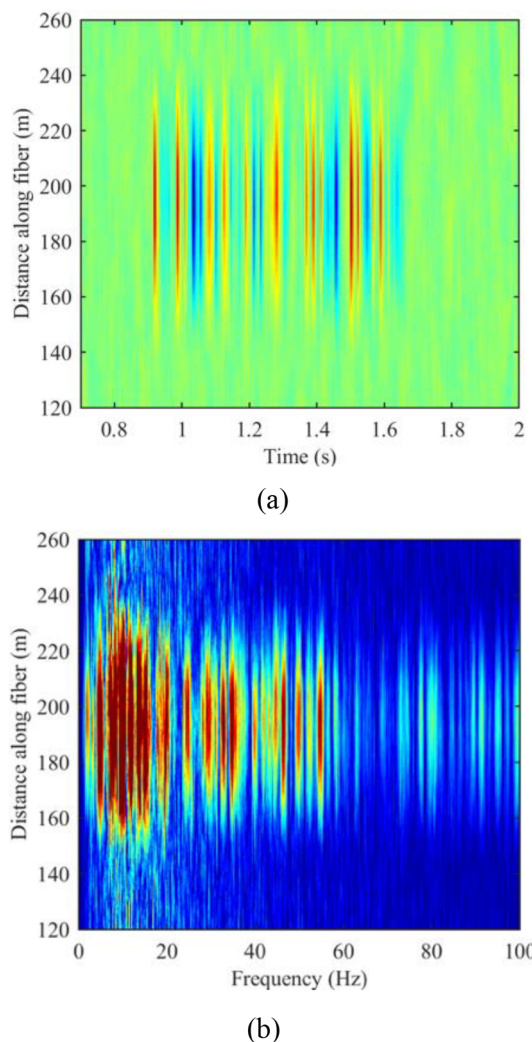


**Fig. 8.** Results of the electric discharge on conductive board experiment. a) Time domain analysis. b) Frequency domain analysis.

## 5. Conclusion

In this work we evaluated the ability of a DOFS vibration sensor based on a Sagnac interferometer to detect and locate electric discharges. Two experiments were carried out over the same fiber but at different positions. In the first experiment, a conductive board with 10 m of optical fiber positioned on its surface was instrumented in a spiral form. In the second experiment, 1.2 m of fiber was positioned parallel to a conductor cable. Due to the high sensitivity the proposed system was able to detect and locate electric discharges in both experiments using the time and frequency domain signals, even with a spatial resolution of approximately 50 m.

The joint analysis of the signals processed in the time and frequency domains allowed the detection of electric discharges and location of the phenomenon within the spatial resolution (50 m). The construction of cables consisting of optical fibers and conducting wires arranged in parallel, similar to what was done in the second experiment, is practical. With this configuration, the distributed detection system based on Sagnac interferometer can be used for predictive maintenance purposes in electric machines instrumented with optical fibers. Some candidate electric machines include motors, generators and transformers. Moreover, the sensing system can be useful in preventing degradation of electrical cables, poor performance or even catastrophic failures.

The high availability and simplicity of low coherence optical sources makes the application of the proposed sensing system feasible

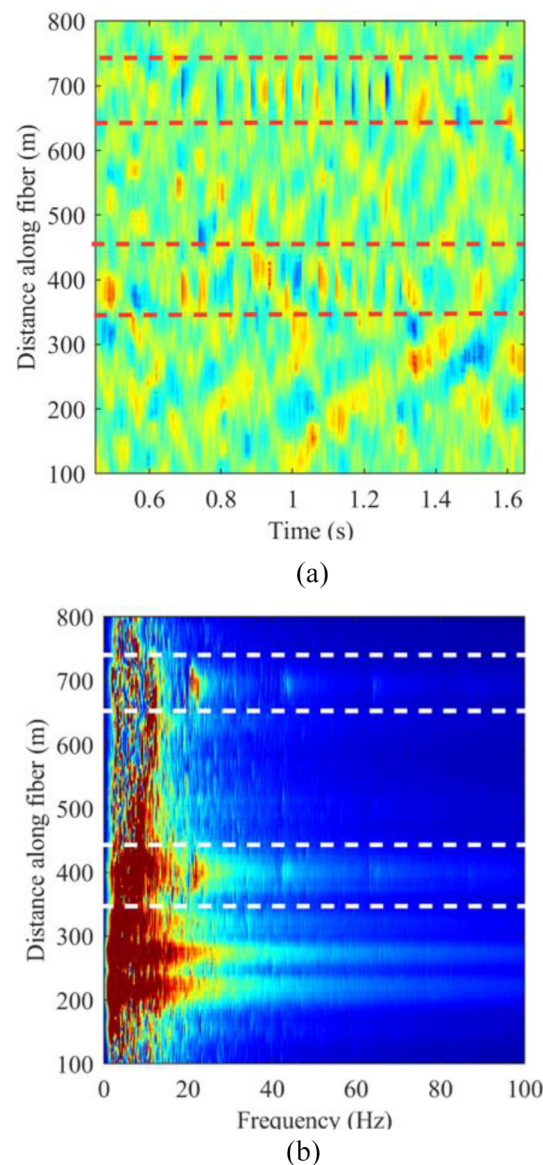


**Fig. 9.** Results of the experiments on insulated electrical cable. a) Time domain analysis. b) Frequency domain analysis.

in such scenarios. It offers opportunities for more detailed studies on recognizing patterns of the vibration signals caused by electric discharges using a distributed vibration sensing system based on Sagnac interferometer.

Finally, some parameters are critical for the measuring capabilities of the sensing system. The sensitivity relies fundamentally on the mechanical stability on the interferometer. Higher quality signals will be detected if more effective vibration insulation of the optical fiber paths is implemented.

## Declaration of Competing Interest

The authors declare that they have no known competing financial interests or personal relationships that could have appeared to influence the work reported in this paper.

## Acknowledgments

The authors acknowledge CAPES (Coordination of Superior Level Staff Improvement), CNPQ (National Council for Scientific and

Technological Development), FINEP (Funding Authority for Studies and Projects), Araucaria Foundation, and SETI (State Secretariat of Science, Technology, and Higher Education of Paraná). This study was financed in part by the Coordenação de Aperfeiçoamento de Pessoal de Nível Superior - Brasil (CAPES) - Finance Code 001.

## References

- [1] F.H. Kreuger, *Partial Discharge Detection in High Voltage Equipment*, Butterworth-Heinemann, 1990.
- [2] J. Mason, Enhancing the significance of PD measurements, *IEEE Trans. Dielectr. Electr. Insul.* 2 (1995) 876–888.
- [3] E. Gulski, Digital analysis of partial discharges, *IEEE Trans. Dielectr. Electr. Insul.* 2 (1995) 822–837.
- [4] J. Ramrez-Nino, R. Mijarez, J.H. Rodriguez, Simple acoustic sensor array for partial discharge detection and location in electrical apparatus, *Meas. Control* 48 (2015) 122–128.
- [5] R. Bartnikas, E. McMahon (Eds.), *Engineering Dielectrics Volume I Corona Measurement and Interpretation*, ASTM International, 1979.
- [6] W. Gao, D. Ding, W. Liu, Research on the typical partial discharge using the UHF detection method for GIS, *IEEE Trans. Power Delivery* 26 (2011) 2621–2629.
- [7] S. Birlasekaran, W.H. Leong, Comparison of known PD signals with the developed and commercial HFCT sensors, *IEEE Trans. Power Delivery* 22 (2007) 1581–1590.
- [8] S. Chakravorti, B. Chatterjee, D. Dey, *Recent Trends in the Condition Monitoring of Transformers*, Springer, London, 2013.
- [9] IEC-62478, High voltage test techniques – Measurement of partial discharges by electromagnetic and acoustic methods, Standard, International Electrotechnical Commission, Geneva, CH, 2016.
- [10] M. MacAlpine, Z. Zhiqiang, M. Demokan, Development of a fibre-optic sensor for partial discharges in oil-filled power transformers, *Electr. Power Syst. Res.* 63 (2002) 27–36.
- [11] J. E. Posada-Roman, J. A. Garcia-Souto, J. R. Serrano, I. B. Nunez, Multichannel ultrasound instrumentation for on-line monitoring of power transformers with internal fiber optic sensors, in: 2013 IEEE International Instrumentation and Measurement Technology Conference (I2MTC), IEEE, 2013.
- [12] B. Sarkar, D.K. Mishra, C. Koley, N.K. Roy, P. Biswas, Intensity-modulated fiber bragg grating sensor for detection of partial discharges inside high-voltage apparatus, *IEEE Sens. J.* 16 (2016) 7950–7957.
- [13] A. Rosenthal, D. Razansky, V. Ntziachristos, High-sensitivity compact ultrasonic detector based on a pi-phase-shifted fiber bragg grating, *Opt. Lett.* 36 (2011) 1833.
- [14] S.E.U. Lima, R.G. Farias, F.M. Araújo, L.A. Ferreira, J.L. Santos, V. Miranda, O. Frazão, Fiber laser sensor based on a phase-shifted chirped grating for acoustic sensing of partial discharges, *Photonic Sensors* 3 (2012) 44–51.
- [15] P. Rohwetter, R. Eisermann, S. Grosswig, K. Krebber, Fibre-optic distributed acoustic and vibration sensing for monitoring of industrial plants and installations, in: *Transforming the Future of Infrastructure through Smarter Information, Proceedings of the International Conference on Smart Infrastructure and Construction, ICSIC, 2016*, 2016, pp. 63–68.
- [16] J. Posada-Roman, J.A. Garcia-Souto, J. Rubio Serrano, Fiber optic sensor for acoustic detection of partial discharges in oil-paper insulated electrical systems, *Sensors* 12 (2012) 4793–4802.
- [17] B. Yu, D.W. Kim, J. Deng, H. Xiao, A. Wang, Fiber fabry-perot sensors for detection of partial discharges in power transformers, *Appl. Opt.* 42 (2003) 3241.
- [18] Y. Wang, X. Li, Y. Gao, H. Zhang, D. Wang, B. Jin, Partial discharge ultrasound detection using the sagnac interferometer system, *Sensors* 18 (2018) 1425.
- [19] C. Pan, X. Liu, H. Zhu, X. Shan, X. Sun, Distributed optical fiber vibration sensor based on sagnac interference in conjunction with otdr, *Opt. Express* 25 (2017) 20056.
- [20] B. Culshaw, The optical fibre sagnac interferometer: an overview of its principles and applications, *Meas. Sci. Technol.* 17 (2005) R1–R16.
- [21] Y. Wang, M. Guo, X. Liu, Q. Bai, D. Wang, M. Zhang, B. Jin, Distributed acoustic sensor based on improved minimum control recursive average algorithm, *Opt. Fiber Technol.* 50 (2019) 125–131.